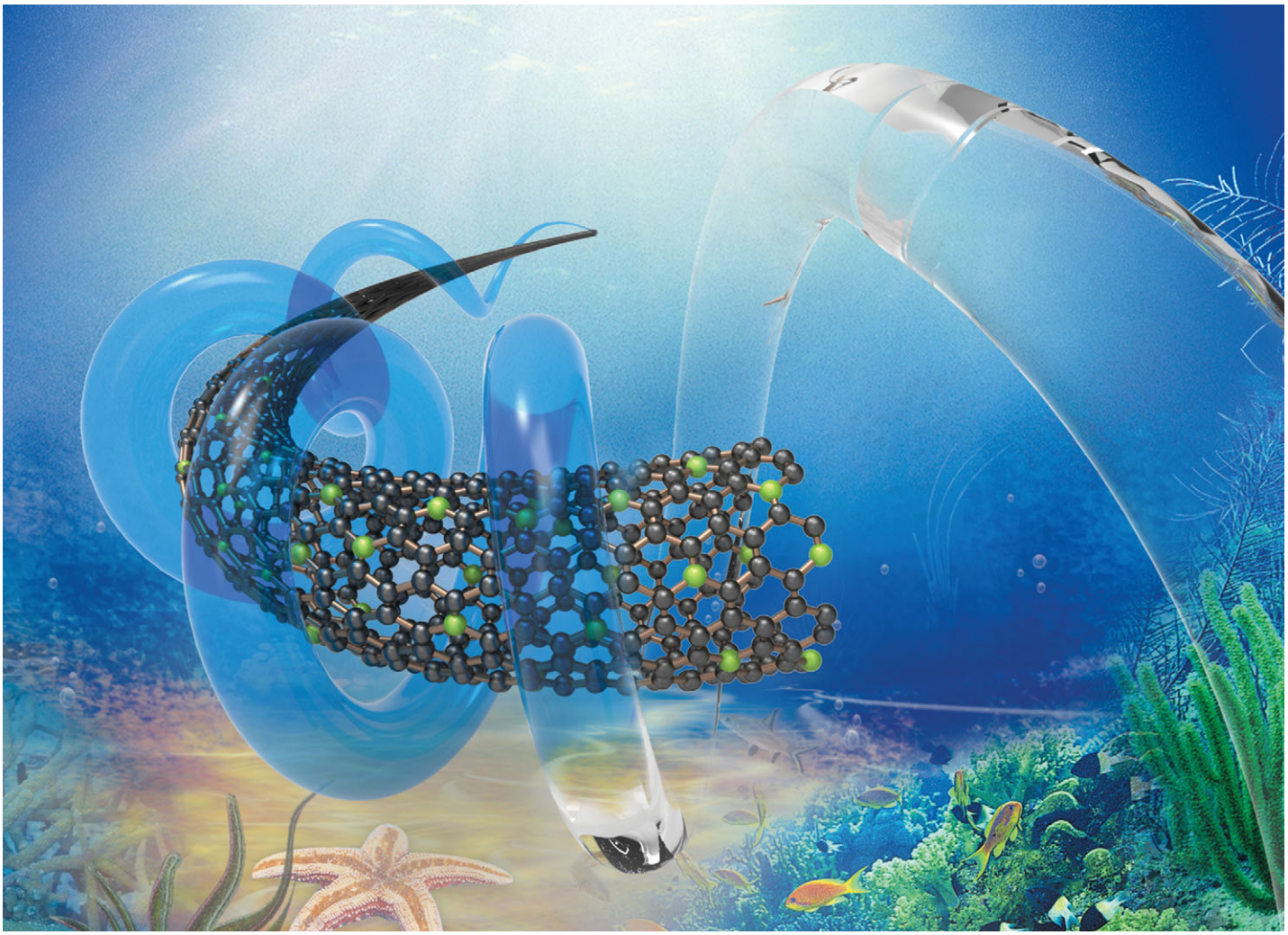

Showcasing research from the group of Professor Shaobin Wang at Department of Chemical Engineering, Curtin University, and Centre for Clean Energy Technology, University of Technology, Sydney, Australia.

Insights into N-doping in single-walled carbon nanotubes for enhanced activation of superoxides: a mechanistic study

Metal free catalysis by N-doped single-walled carbon nanotubes in activation of hydrogen peroxide, persulfate, and peroxymonosulfate for advanced oxidation process was investigated by experiments and theoretical calculations, which provides first insights into carbocatalysis for organic oxidation in sustainable remediation.

As featured in:

See Hongqi Sun, Shaobin Wang *et al.*, *Chem. Commun.*, 2015, **51**, 15249.

ROYAL SOCIETY OF CHEMISTRY

www.rsc.org/chemcomm

Registered charity number: 207890

ChemComm

COMMUNICATION

View Article Online
View Journal | View Issue

Cite this: *Chem. Commun.*, 2015, **51**, 15249

Received 22nd June 2015,
Accepted 10th August 2015

DOI: 10.1039/c5cc05101k

www.rsc.org/chemcomm

Insights into N-doping in single-walled carbon nanotubes for enhanced activation of superoxides: a mechanistic study†

Xiaoguang Duan,[a] Zhimin Ao,[b] Hongqi Sun,*[a] Li Zhou,[a] Guoxiu Wang[b] and Shaobin Wang*[a]

Emerging characteristics upon nitrogen-doping were differentiated in the activation of superoxides over single-walled carbon nanotubes. Both experimental and theoretical studies revealed that enhanced peroxymonosulfate (PMS) activation is ascribed to a nonradical process while persulfate (PS) activation is accelerated *via* directly oxidizing water, yet hydrogen peroxide (H_2O_2) activation is inert to N-doping. This study details the first insights into versatile N-doping in carbocatalysis for organic oxidation in sustainable remediation.

In recent years, water pollution has become one of the key issues in environmental deterioration which triggers worldwide concerns. Sustainable water resources from domestic sewage and industrial wastewater can be exploited through advanced oxidative processes (AOPs). Various superoxides such as ozone (O_3), hydrogen peroxide (H_2O_2), persulfate ($S_2O_8^{2-}$, PS), and peroxymonosulfate (HSO_5^-, PMS) are activated to produce reactive radicals to decompose toxic organic compounds into carbon dioxide, water and mineralized acids. For example, conventional Fenton reactions employ ferrous ions as an efficient homogeneous catalyst to activate H_2O_2 to generate hydroxyl radicals. However, this process requires strict acidic conditions (pH $\sim$ 3) and produces a lot of sludge due to coagulation.[1] Metal-based heterogeneous catalysts, such as MnO_2,[2] CuO,[3] $CuFe_2O_4$,[4] and zerovalent iron (ZVI),[5] have been used to activate PMS and PS to conduct sulfate radical based oxidation, yet the stubborn toxic metal leaching severely limits the future practical applications.

Emerging carbocatalysis is able to completely avoid the secondary contamination from metal leaching owing to its metal-free nature.[6,7] However, the efficiencies of pristine nanocarbons in the activation of superoxides are very low. We first discovered that reduced graphene oxide (rGO) can effectively activate PMS and further proved that nitrogen doping can remarkably enhance the catalytic oxidation.[8,9] Heteroatom doping can effectively break the inertness of the graphene carbon matrix and induce novel physicochemical and electronic properties for enhanced catalysis.[10–15] More recently, we observed that nitrogen-doping would induce a non-radical pathway in catalytic oxidation with PMS.[16,17] However, the origin of the emerging features from nitrogen doping is not clear in PMS activation yet, and is even more blurred in PS and H_2O_2 activation.

In this study, experimental results and theoretical calculations are integrated to reveal the effect of nitrogen doping on the radical generation processes over single-walled carbon nanotubes (SWCNTs). The pristine SWCNTs were thoroughly refluxed in concentrated nitric acid to remove any potential metal impurities (denoted as o-SWCNTs). The purified o-SWCNTs were then heated at 700 °C in N_2 to remove excess functional groups (denoted as SWCNTs-700), or annealed with melamine as a N-precursor to produce the nitrogen-doped sample (denoted as N-SWCNTs).[17] The physical and chemical properties of the prepared carbocatalysts are displayed in Table S1 (ESI†). The nitrogen modified SWCNTs were designed with a highly crystallized structure (I_D/I_G = 0.35) and a low oxygen level (1.15 at%) to minimize the system complexity from defects and functional groups. The effect of nitrogen doping on the activation of PMS, PS, and H_2O_2 was evaluated by phenol oxidation.

Fig. 1 shows that the super-oxidants can hardly oxidize phenol without a catalyst. The catalytic performance of the modified SWCNTs for PMS activation is illustrated in Fig. 1a. The o-SWCNTs can provide 56.5% phenol removal in 180 min, while SWCNTs-700 and N-SWCNTs achieved complete phenol degradation in 180 and 45 min, respectively.[17] The initial reaction rates of o-SWCNTs, SWCNTs-700, and N-SWCNTs were calculated to be 0.09, 0.46, and 4.93 ppm min^{-1}, respectively, based on pseudo first-order kinetics. The observations on carbon nanotubes-based materials were consistent with those of rGO, which was more efficient for PMS activation than GO

[a] *Department of Chemical Engineering, Curtin University, GPO Box U1987, Perth, WA 6845, Australia. E-mail: Shaobin.wang@curtin.edu.au, h.sun@curtin.edu.au*
[b] *Centre for Clean Energy Technology, School of Mathematical and Physical Sciences, University of Technology Sydney, PO Box 123, Broadway, Sydney, NSW 2007, Australia*

† Electronic supplementary information (ESI) available: EPR spectra, theoretical calculation details. See DOI: 10.1039/c5cc05101k

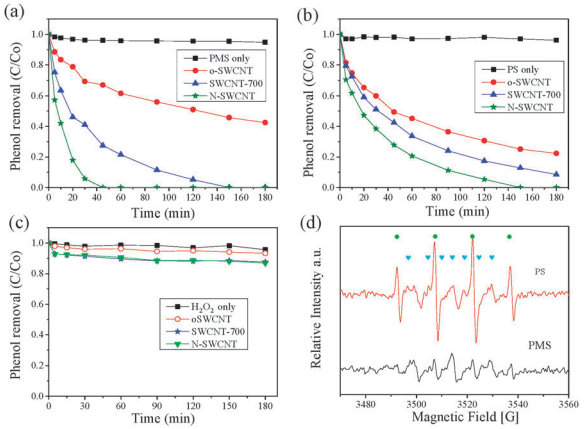

Fig. 1 Phenol oxidation with (a) PMS (6.5 mM), (b) PS (6.5 mM) and (c) H_2O_2 (30 mM) under various conditions. [Phenol] = 20 ppm, [catalyst] = 0.1 g L^{-1}, [temperature] = 25 °C. (d) EPR spectra of PMS and PS activation on N-SWCNTs (●: DMPO–OH, ♥: DMPO–SO_4).

with excess oxygen groups but less active than nitrogen doped rGO.[8,9,16] We further combined experimental design and computational studies to reveal that substitutional N-doping (graphitic N) can effectively break the chemical inertness of the conjugated graphene network and facilitate charge transfer from adjacent carbon atoms to graphitic nitrogen atoms, giving rise to positively charged sites which can effectively improve the adsorption capability of PMS and weaken the O–O (HO–SO_4) bond.[16,18] The influence of the annealing temperature of N-SWCNTs on PS activation was illustrated in Fig. S2 (ESI†). N-SWCNTs obtained at 700 °C present the best catalytic activity, which is consistent with our previous studies on PMS activation on N-rGO and N-SWCNTs.[16,17] Raising the temperature results in a lower N concentration owing to the breakup of C–N bonds, meanwhile attaining a higher graphitic N proportion due to its better thermal stability. The experimental results suggest that both the N-doping level and nitrogen species synergistically affect the carbocatalysis for peroxide activation. Additionally, the stability of the carbocatalysts was evaluated as shown in Fig. S3 (ESI†). The N-SWCNTs in the 2nd and 3rd cycles provided 73.2% and 53.0% phenol removal, respectively. The deactivation of the carbocatalysts can be ascribed to the alteration of surface charges and the detachment of N dopants during the oxidation processes.

N-doping for potentially enhanced PS and H_2O_2 activation is presented in Fig. 1b and c. It was found that N-doping can slightly improve the catalytic performance in PS activation, however, it is ineffective for H_2O_2 activation. More specifically, o-SWCNTs, SWCNTs-700, and N-SWCNTs attained 77.8, 91.6, and 100% phenol degradation with PS in 180 min and the initial reaction rates were estimated to be 0.32, 0.42, and 0.60 ppm min^{-1} accordingly. It is interesting to note that, though o-SWCNTs are more efficient for PS activation than PMS, the nitrogen-doped sample does not show the same trend, suggesting that the intrinsic mechanism of PS and PMS activation on N-SWCNTs might be different. Fig. 1c indicates poor effectiveness for H_2O_2 activation on both SWCNTs-700 and N-SWCNTs with only 12.3 and 13.1% phenol oxidation in 180 min, compared with 6.7% phenol removal on o-SWCNTs. Recently, Yang *et al.* reported that ozone can react with PMS to generate sulfate and hydroxyl radicals,[19] which motivated us to explore if such a synergistic effect exists in the PMS/H_2O_2 or PS/H_2O_2 systems. However, as illustrated in Fig. S4 (ESI†), we found that both PMS and PS cannot work as efficient initiators to improve the activation of H_2O_2 on N-SWCNTs. Moreover, the presence of H_2O_2 lowered the phenol oxidation efficiency on PMS/N-SWCNTs and PS/N-SWCNTs.

We employed *in situ* electron paramagnetic resonance (EPR) to investigate the radical generation process during PMS and PS activation on the carbocatalysts. As the generated free radicals usually have a very short lifetime and then quickly react with the organic compounds or are quenched through coupling with another radical molecule, the free-radicals were captured by a spin-trapping agent, 5,5-dimethyl-1-pyrroline *N*-oxide (DMPO), to form relatively stable adducts and detected by EPR for the mechanistic study. As illustrated in Fig. 1d and Fig. S5 (ESI†), N-SWCNTs can activate both PMS and PS to generate sulfate radicals ($SO_4^{\bullet-}$) and hydroxyl radicals ($^{\bullet}OH$). Nevertheless, the PMS/N-SWCNT system is much more efficient than PS/N-SWCNT for phenol oxidation, the intensity of generated radicals from the PS activation is much higher than that from PMS. In the AOPs, the reactive radicals play crucial roles in attacking and decomposing organics into oxidated products. The intrinsic distinction of PMS and PS activation on N-SWCNTs for radical generation and phenol oxidation implies completely different reaction pathways.

We further carried out density functional theory (DFT) calculations to discover the intricate interactions between the superoxides and carbocatalysts. The corresponding O–O bond lengths (l'_{O-O}) in free PMS, H_2O_2 and PS are 1.326, 1.471, and 1.222 Å, respectively. Table 1 suggests that the adsorption of PMS and PS on both the SWCNTs and N-doped SWCNTs is quite strong, which induces a relatively large electron transfer between the oxidant molecules and the SWCNTs (or N-SWCNTs). The O–O bond length (l_{O-O}) of SO_3–OH in PMS and SO_4–SO_4 in PS increased remarkably comparing with that of free PMS and PS. However, the adsorption of H_2O_2 is very weak, mirrored by the low adsorption energy and near zero charge transfer. Therefore, SWCNTs are theoretically proven to have excellent

Table 1 The adsorption energy E_{ads}, electron transfer between SWCNTs and the adsorbed molecule Q, and the O–O bond length (l_{O-O}) of SO_3–OH in PMS, SO_4–SO_4 in PS, and HO–OH in H_2O_2 from different adsorption configurations in Fig. S6 (ESI)

Type of CNT	Molecules	E_{ads} (eV)	Q (e)	l_{O-O} (Å)
Free molecule	PMS	—	—	1.326
	PS	—	—	1.222
	H_2O_2	—	—	1.471
SWCNTs	PMS	−2.05	−0.455	1.402
	PS	−1.74	−0.693	1.295
	H_2O_2	−0.30	0	1.469
N-doped SWCNTs	PMS	−2.98	−0.757	1.459
	PS	−2.99	−0.945	1.344
	H_2O_2	−0.26	0.007	1.471

performance to activate PMS and PS molecules and make them be dissociated into $-SO_3$ and –OH groups, or two $-SO_4$ groups. The noticeable electron transfer tendency (Q) possibly suggests the generation of free radicals and anions. After N incorporation into the SWCNTs, the catalytic performance increases with a higher adsorption energy, more rapid charge transfer, and larger l_{O-O} value. Such changes were not observed in H_2O_2 activation. Thus, the theoretical findings are in good accordance with the experimental results.

Nevertheless the calculations revealed that nitrogen doping has a more remarkable enhancement for PS activation than PMS (reflected by more significant increases in E_{ads}, Q, and l_{O-O}), the catalytic oxidation did not follow this theoretical expectation. Based on the experiments and DFT calculations, we suggest that PMS and PS activation processes on N-SWCNTs might be different. In a previous study, we first discovered that N-doping can induce nonradical reactions which co-exist with the radical pathway during catalytic phenol oxidation with PMS.[17] The PMS molecules are first adsorbed and interact with an activated sp^2-conjugated carbon network due to nitrogen-doping, and then react rapidly with the target organics *via* a nonradical-generated oxidation process. The same phenomenon was also found in a PS/CuO system. PS first interacts with the outer-sphere of CuO electronic shell, which is the rate-limiting step, and then decomposes 2,4-chlorophenol directly.[3] In order to investigate if such non-radical processes occur in the PS/N-SWCNT system as well, ethanol (EtOH), which can quickly quench both the sulfate and hydroxyl radicals, was utilized as a radical scavenger to quench the reactive species produced from PS activation.[20] The phenol degradation efficiency decreased significantly with the rising ratio of ethanol in the PS/SWCNT-700 and PS/N-SWCNT systems (Fig. 2a and b). The initial reaction rates were estimated (Fig. 2c) and reduced significantly when the water was completely replaced by ethanol (only around 1% water remaining introduced during preparation of phenol solution), which is intrinsically different from the PMS/N-SWCNT system in which very high phenol removal efficiency was maintained in the ethanol solution.[17] The oxidation reaction was almost terminated at high concentration of ethanol in the PS/N-SWCNT systems, suggesting that the generation of reactive radicals was essential for phenol oxidation with PS and the non-radical process was almost absent in the PS/N-SWCNT system.

It is also noteworthy that N-SWCNTs can effectively activate PS to generate large amounts of hydroxyl radicals (•OH) as indicated in the EPR spectra (Fig. 1d). To the best of our knowledge, persulfate ($S_2O_8^{2-}$) cannot generate hydroxyl radicals itself and the large amounts of hydroxyl radicals can exclusively be devolved from water. We suppose that PS might be able to oxidize water directly on N-SWCNTs to generate hydroxyl radicals for phenol degradation, shown in Fig. 2d. A theoretical model was built up to modulate this process as presented in Fig. 3a and b. As one can see from Fig. 3c and Table S2 (ESI†), the adsorption of H_2O molecules on the nitrogen-doped SWCNTs is minor due to the weak adsorption energy, little electron transfer from H_2O to SWCNTs, and the O–H bond length rarely changes after adsorption. However, if a PS molecule presents together with a water molecule on the N-SWCNTs (Fig. 3b), the H_2O molecule adsorption enhances remarkably, where the adsorption energy increases by almost 3 times, the charge transfer becomes 7 times faster, and the O–H bond length is also prolonged greatly (Table S2, ESI†). The adsorption capability of PS is also enhanced with a longer O–O bond length and faster electron transfer (Fig. 3d). Therefore, the presence of PS can promote the dissociation of H_2O and facilitate the generation of –OH groups to form hydroxyl radicals. N-doped carbon nanotubes can activate H_2O molecules *via* acting as a facilitating bridge for electron transfer from H_2O to PS as proposed in Fig. 2d. Besides, PS might be converted into sulfate ions directly due to its great ability to extract electrons from the carbon matrix on N-SWCNTs (Fig. 3d and Table S2, ESI†) when

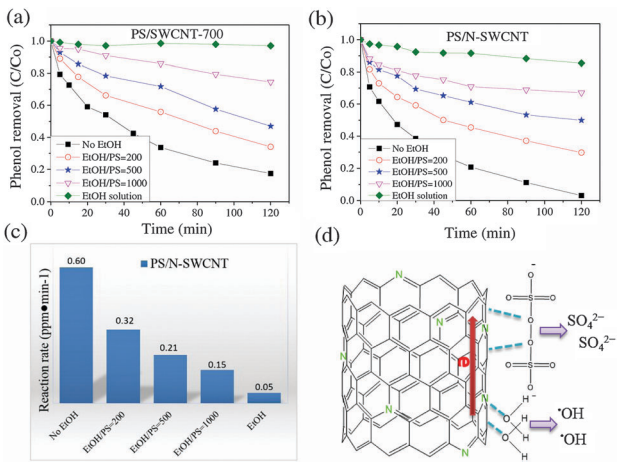

Fig. 2 Effects of radical scavenger (EtOH) on phenol degradation in (a) PS/SWCNT-700, and (b) PS/N-SWCNT systems. (c) Reaction rates of phenol oxidation with PS on N-SWCNTs under different ratios of EtOH. ([Phenol] = 20 ppm, [catalyst] = 0.1 g L^{-1}, [temperature] = 25 °C, [PS] = 6.5 mM.) (d) Proposed mechanism of PS activation on N-SWCNTs.

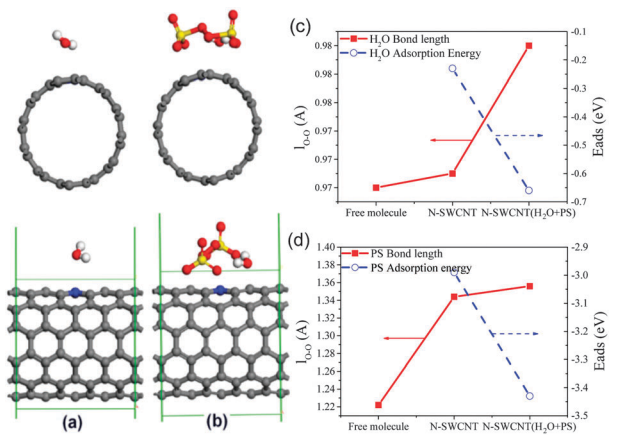

Fig. 3 (a) H_2O adsorption on N-SWCNTs, (b) PS and H_2O adsorbed on the N-SWCNTs. (The grey, blue, red, yellow, and white atoms are C, N, O, S, and H atoms, respectively.) The O–O bond length (l_{O-O}) and adsorption energy of (c) H_2O and (d) PS under different conditions: free molecule, adsorption alone on N-SWCNTs, and co-adsorbed on N-SWCNTs.

they co-exist with adsorbed water, as no obvious signal of sulfate radicals can be found in the EPR spectra in Fig. 1d. Distinct from PS and H_2O_2, the asymmetric structure of PMS (HO–SO_4) and the relatively weak adsorption and oxidation ability on N-SWCNTs might contribute to the emerging nonradical reaction for PMS activation.

In summary, we investigated the effect of N-doping on the activation of various superoxides including PMS, PS, and H_2O_2. Both experimental results and theoretical calculations proved that N-doping can enhance PMS and PS activation, yet it is not effective for H_2O_2 activation. N-doping can induce nonradical oxidation in PMS activation, whereas it works as an excellent electron-bridge to facilitate PS to oxidize adsorbed water to generate hydroxyl radicals for catalytic oxidation. This study concludes new insights into N-doping in carbocatalysis for oxidative processes in the aqueous phase.

This work was financially supported by Australian Research Council under project No. DP130101319. Computational study was supported by the National Computational Infrastructure (NCI) through the merit allocation scheme and used NCI resources and facilities in Canberra, Australia. H. S. acknowledges Curtin Research Fellowship and opening project (KL-13 02).

Notes and references

1 X. W. Liu, X. F. Sun, D. B. Li, W. W. Li, Y. X. Huang, G. P. Sheng and H. Q. Yu, *Water Res.*, 2012, **46**, 4371–4378.
2 E. Saputra, S. Muhammad, H. Sun, H. M. Ang, M. O. Tade and S. Wang, *Environ. Sci. Technol.*, 2013, **47**, 5882–5887.
3 T. Zhang, Y. Chen, Y. Wang, J. Le Roux, Y. Yang and J.-P. Croué, *Environ. Sci. Technol.*, 2014, **48**, 5868–5875.
4 T. Zhang, H. Zhu and J.-P. Croue, *Environ. Sci. Technol.*, 2013, **47**, 2784–2791.
5 P. Drzewicz, L. Perez-Estrada, A. Alpatova, J. W. Martin and M. G. El-Din, *Environ. Sci. Technol.*, 2012, **46**, 8984–8991.
6 W. Cui, Q. Liu, N. Y. Cheng, A. M. Asiri and X. P. Sun, *Chem. Commun.*, 2014, **50**, 9340–9342.
7 N. Y. Cheng, Q. Liu, J. Q. Tian, Y. R. Xue, A. M. Asiri, H. F. Jiang, Y. Q. He and X. P. Sun, *Chem. Commun.*, 2015, **51**, 1616–1619.
8 H. Q. Sun, S. Z. Liu, G. L. Zhou, H. M. Ang, M. O. Tade and S. B. Wang, *ACS Appl. Mater. Interfaces*, 2012, **4**, 5466–5471.
9 H. Q. Sun, Y. X. Wang, S. Z. Liu, L. Ge, L. Wang, Z. H. Zhu and S. B. Wang, *Chem. Commun.*, 2013, **49**, 9914–9916.
10 Y. Kim and S. Shanmugam, *ACS Appl. Mater. Interfaces*, 2013, **5**, 12197–12204.
11 J. Sanetuntikul, T. Hang and S. Shanmugam, *Chem. Commun.*, 2014, **50**, 9473–9476.
12 Z.-S. Wu, S. Yang, Y. Sun, K. Parvez, X. Feng and K. Muellen, *J. Am. Chem. Soc.*, 2012, **134**, 9082–9085.
13 Y. Li, Y. Zhao, H. Cheng, Y. Hu, G. Shi, L. Dai and L. Qu, *J. Am. Chem. Soc.*, 2012, **134**, 15–18.
14 S. Y. Wang, L. P. Zhang, Z. H. Xia, A. Roy, D. W. Chang, J. B. Baek and L. M. Dai, *Angew. Chem., Int. Ed.*, 2012, **51**, 4209–4212.
15 J. Liang, Y. Jiao, M. Jaroniec and S. Z. Qiao, *Angew. Chem., Int. Ed.*, 2012, **51**, 11496–11500.
16 X. G. Duan, Z. M. Ao, H. Q. Sun, S. Indrawirawan, Y. X. Wang, J. Kang, F. L. Liang, Z. H. Zhu and S. B. Wang, *ACS Appl. Mater. Interfaces*, 2015, **7**, 4169–4178.
17 X. G. Duan, H. Q. Sun, Y. X. Wang, J. Kang and S. B. Wang, *ACS Catal.*, 2015, **5**, 553–559.
18 X. G. Duan, K. O'Donnell, H. Q. Sun, Y. X. Wang and S. B. Wang, *Small*, 2015, **11**, 3036–3044.
19 Y. Yang, J. Jiang, X. L. Lu, J. Ma and Y. Z. Liu, *Environ. Sci. Technol.*, 2015, **49**, 7330–7339.
20 G. P. Anipsitakis and D. D. Dionysiou, *Environ. Sci. Technol.*, 2003, **37**, 4790–4797.

